

Elastic Deformation of Membrane Bilayers Probed by Deuterium NMR Relaxation

Michael F. Brown,^{*,†,‡} Robin L. Thurmond,^{†,§} Steven W. Dodd,^{†,||} Dörte Otten,[⊥] and Klaus Beyer[⊥]

Contribution from the Department of Chemistry, University of Arizona, Tucson, Arizona 85721, and Lehrstuhl für Stoffwechselbiochemie, Universität München, D-80336 München, Germany

Received December 4, 2001

Abstract: In deuterium (^2H) NMR spectroscopy of fluid lipid bilayers, the average structure is manifested in the segmental order parameters (S_{CD}) of the flexible molecules. The corresponding spin–lattice relaxation rates (R_{1Z}) depend on both the amplitudes and the rates of the segmental fluctuations, and indicate the types of lipid motions. By combining ^2H NMR order parameter measurements with relaxation studies, we have obtained a more comprehensive picture of lipids in the liquid-crystalline (L_{α}) state than formerly possible. Our data suggest that a lipid bilayer constitutes an ordered fluid, in which the phospholipids are grafted to the aqueous interface via their polar headgroups, whereas the fatty acyl chains are in effect liquid hydrocarbon. Studies of ^2H -labeled saturated lipids indicate their R_{1Z} rates and S_{CD} order parameters are correlated by a model-free, square-law functional dependence, signifying the presence of relatively slow bilayer fluctuations. A new composite membrane deformation model explains simultaneously the frequency (magnetic field) dependence and the angular anisotropy of the relaxation. The results imply the R_{1Z} rates are due to a broad spectrum of 3-D collective bilayer excitations, together with effective axial rotations of the lipids. For the first time, NMR relaxation studies show that the viscoelastic properties of membrane lipids at megahertz frequencies are modulated by the lipid acyl length (bilayer thickness), polar headgroups (bilayer interfacial area), inclusion of a nonionic detergent (C_{12}E_8), and the presence of cholesterol, leading to a range of bilayer softness. Our findings imply the concept of elastic deformation is relevant on lengths approaching the bilayer thickness and less (the mesoscopic scale), and suggest that application of combined R_{1Z} and S_{CD} studies of phospholipids can be used as a simple membrane elastometer. Heuristic estimates of the bilayer bending rigidity κ and the area elastic modulus K_a enable comparison to other biophysical studies, involving macroscopic deformation of thin membrane lipid films. Finally, the bilayer softness may be correlated with the lipid diversity of biomembranes, for example, with regard to membrane curvature, repulsive interactions between bilayers, and lipid–protein interactions.

Introduction

Studies of membrane lipids are important in structural genomics, nanotechnology, and biosensor development, and from a fundamental viewpoint as smectic liquid-crystalline materials. A substantial fraction of the coding sequences of the human genome involve membrane proteins, whose interactions with lipid bilayers can affect their structural properties and biological activities. In several instances it has been shown that the activities of integral membrane proteins and membrane-spanning peptides depend on the nature of the surrounding phospholipid bilayer.^{1–3} The deformability of membrane bilayers

has also attracted increased attention^{1,4} on account of the connection to lipid-mediated functions of proteins in biomembranes,¹ interbilayer interactions,^{5,6} and membrane fusion.⁷ Consequently, it is desirable to study the biophysical properties of membrane constituents on length scales commensurate to those of the lipids and the embedded protein and peptide molecules.

There are two complementary strategies for investigating the deformations of liquid-crystalline membrane films. One possibility is to study the static deformation of the bilayer from equilibrium, due to application of an external field.⁵ An alternative is to investigate the spontaneous bilayer fluctuations associated with random thermal forces.^{8,9} The same material

* To whom correspondence should be addressed. Phone: 520-621-2163. Fax: 520-621-8407. E-mail: mfbrown@u.arizona.edu.

† University of Arizona.

‡ Additional address: Universität Würzburg, Physikalisches Institut EP-5, D-97074 Würzburg, Germany.

§ Present address: R.W. Johnson Pharmaceutical Research Institute, 3210 Merryfield Road, San Diego, CA 92121.

|| Present address: Eli Lilly and Company, Lilly Research Laboratories, Pharmaceutical Research and Development, Lilly Corporate Center, Indianapolis, IN 46285.

⊥ Universität München.

(1) Brown, M. F. *Chem. Phys. Lipids* **1994**, *73*, 159–180.

(2) Lee, A. G. *Biochim. Biophys. Acta* **1998**, *1376*, 381–390.

(3) Epanand, R. M. *Biochim. Biophys. Acta* **1998**, *1376*, 353–368.

(4) Bloom, M.; Evans, E.; Mouritsen, O. G. *Q. Rev. Biophys.* **1991**, *24*, 293–397.

(5) Evans, E.; Needham, D. *J. Phys. Chem.* **1987**, *91*, 4219–4228.

(6) Israelachvili, J. N.; Wennerström, H. *J. Phys. Chem.* **1992**, *96*, 520–531.

(7) Peisajovich, S. G.; Epanand, R. F.; Pritsker, Y.; Shai, Y.; Epanand, R. M. *Biochemistry* **2000**, *39*, 1826–1833.

(8) Sackmann, E. In *Handbook of Biological Physics*; Lipowsky, R., Sackmann, E., Eds.; Elsevier: Amsterdam, 1995; Vol. 1, pp 213–304.

(9) Hirn, R.; Benz, R.; Bayerl, T. M. *Phys. Rev. E* **1999**, *59*, 1–8.

constants describe the deformations of the membrane in either case. Here, nuclear magnetic resonance (NMR)¹⁰ spectroscopy provides a useful means of studying both the equilibrium properties and the dynamics of membrane constituents. In solid-state NMR, the line shapes provide an understanding of the average structure of the membrane, as characterized by motional averaging of the coupling tensors (quadrupolar, dipolar, chemical shift) of the various nuclei.^{4,11,12} A distinctive feature of NMR spectroscopy, for example, as compared to X-ray and neutron scattering studies, is that the nuclear spin relaxation rates give knowledge of the dynamics of the system, as manifested by fluctuations of the nuclear coupling tensors.^{12,13} By combining solid-state NMR measurements with relaxation studies, a more complete picture can be obtained than with either approach alone.

For instance, a fundamental question with regard to soft biomembrane systems concerns how the microscopic structural and dynamical information from NMR spectroscopy is related to their properties on the mesoscopic length scale (about the bilayer thickness and less). At what point does one relinquish a macroscopic, continuum treatment of the bulk material, which ignores the molecules altogether—in favor of curvature or area elasticity—and introduce molecular properties of the constituents? The hypothesis of local elastic deformation as an explanation for the nuclear spin–lattice relaxation rates of lipid bilayers was first proposed at a conference at Stanford University,¹⁴ and has been subsequently elaborated.^{13,15,16} Previous interpretations had involved either local segmental motions of the lipids¹⁷ or trans–gauche isomerizations together with molecular reorientations.^{18,19} On the basis of solid-state deuterium (²H) NMR studies, we have postulated that a continuum of elastic deformations is present in membrane bilayers, due to a hierarchical superposition of motional processes. Further, we have proposed that elastic distortion of bilayers is applicable on the mesoscopic length scale, with a broad spectrum of modes whose Fourier components range down to the bilayer hydrocarbon thickness and even less.^{15,16} Analogous conclusions have been drawn from recent molecular dynamics simulations of amphiphilic bilayers.^{20,21}

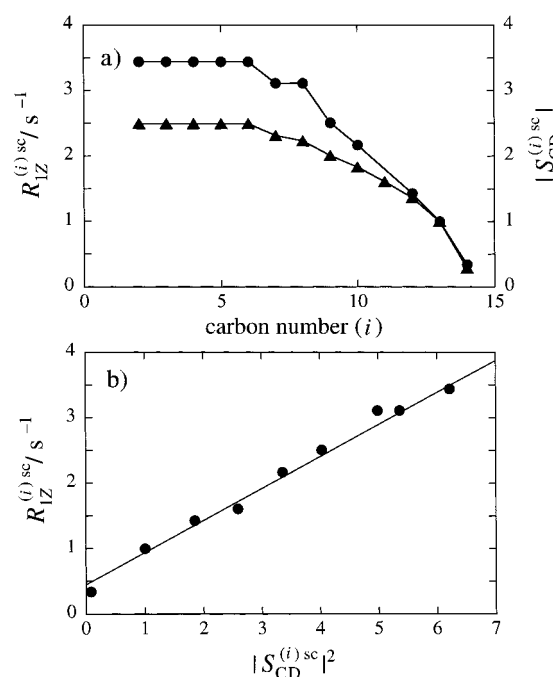


Figure 1. Spin–lattice relaxation rates and C–²H bond segmental order parameters for DMPC-*d*₅₄ in the fluid L_{α} state at 40 °C. Data at 76.8 MHz (11.8 T) are for bilayers of DMPC-*d*₅₄ aligned at $\theta = 90^\circ$, containing 50 wt % H₂O (20 mM Tris buffer, 1 mM EDTA, pH 7.3). The values are scaled at the penultimate ($\omega - 1$) carbon to illustrate their functional dependence. (a) Profiles of scaled (sc) relaxation rates $R_{1Z}^{(i)sc}$ (●) and scaled order parameters $|S_{CD}^{(i)sc}|$ (▲), evincing the steeper dependence of the former on the acyl chain position (index i). (b) Plot of $R_{1Z}^{(i)sc}$ values versus $|S_{CD}^{(i)sc}|^2$, showing dependence of the relaxation function on the square of the order function. The square-law functional dependence is model-free. The data imply that rapid segmental motions of the lipids set up a local order profile, which is subject to slower collective deformations of the bilayer.

In ²H NMR spectroscopy of liquid-crystalline lipid bilayers, the experimental observables comprise the order parameters (S_{CD}) and the spin–lattice relaxation rates (R_{1Z}) as a function of acyl position (i). Hence one can ask: are the relaxation and order functions independent, or rather are they correlated through their dependence on some underlying variables? A closer look at the NMR data for disaturated lipid bilayers reveals that within the hydrocarbon interior, the order function $|S_{CD}^{(i)}|$ and the relaxation function $R_{1Z}^{(i)}$ are not linearly related. Rather, the dependence of the relaxation rates $R_{1Z}^{(i)}$ on the chain position (i) is more pronounced than for the order profile $|S_{CD}^{(i)}|$. As an illustration, consider Figure 1a, in which the relaxation rate profile $R_{1Z}^{(i)}$ and order profile $|S_{CD}^{(i)}|$ for DMPC-*d*₅₄ bilayers are scaled at the penultimate ($\omega - 1$) carbon, and are superimposed to reveal the steeper dependence on acyl segment position in the former case. Numerical fitting of such data to a power law¹⁵ indicates that the segmental $R_{1Z}^{(i)}$ rates scale nearly with the square of the segmental order parameters $|S_{CD}^{(i)}|$ along the chain, with a relatively small ordinate intercept. Such a square-law functional dependence is shown in Figure 1b for DMPC-*d*₅₄ bilayers. Here, the scaled $R_{1Z}^{(i)}$ rates along the acyl chains are plotted versus the square of the corresponding scaled $|S_{CD}^{(i)}|$ order parameters. The observed square-law dependence constitutes a signature of relatively slow motions that modulate the local structure of the bilayer set up by faster trans–gauche rotational isomerization. We have argued that the relatively slow

- (10) Abbreviations used: C₁₂E₈, octaethyleneglycol-mono-*n*-dodecyl ether; DLPC-*d*₄₆, 1,2-diperdeuteriolauroyl-*sn*-glycero-3-phosphocholine; DMPC-*d*₅₄, 1,2-diperdeuteriomyristoyl-*sn*-glycero-3-phosphocholine; DPPC, 1,2-dipalmitoyl-*sn*-glycero-3-phosphocholine; DPPC-*d*₆₂, 1,2-diperdeuteriopalmitoyl-*sn*-glycero-3-phosphocholine; DSPC-*d*₇₀, 1,2-diperdeuteriostearyl-*sn*-glycero-3-phosphocholine; DPPE, 1,2-dipalmitoyl-*sn*-glycero-3-phosphoethanolamine; DPPE-*d*₆₃, 1,2-diperdeuteriopalmitoyl-*sn*-glycero-3-phosphoethanolamine; EDTA, ethylenediaminetetraacetic acid; EFG, electric field gradient; NMR, nuclear magnetic resonance; ODF, order-director fluctuations; PC, phosphocholine or phosphatidylcholine; PE, phosphoethanolamine or phosphatidylethanolamine; R_{1Z} , spin–lattice (Zeeman) relaxation rate; S_{CD} , order parameter of C–²H bond.
- (11) Ruocco, M. J.; Siminovich, D. J.; Long, J. R.; Das Gupta, S. K.; Griffin, R. G. *Biophys. J.* **1996**, *71*, 1776–1788.
- (12) Brown, M. F. In *Biological Membranes. A Molecular Perspective from Computation and Experiment*; Merz, K. M., Jr., Roux, B., Eds.; Birkhäuser: Basel, 1996; pp 175–252.
- (13) Brown, M. F.; Chan, S. I. In *Encyclopedia of Nuclear Magnetic Resonance*; Grant, D. M., Harris, R. K., Eds.; Wiley: New York, 1996; Vol. 2, pp 871–885.
- (14) Brown, M. F. *Proc. Fifth Annual Conference on Molecular Structural Methods in Biological Research*; Stanford University, 1979.
- (15) Brown, M. F. *J. Chem. Phys.* **1982**, *77*, 1576–1599.
- (16) Brown, M. F.; Ribeiro, A. A.; Williams, G. D. *Proc. Natl. Acad. Sci. U.S.A.* **1983**, *80*, 4325–4329.
- (17) Brown, M. F.; Seelig, J.; Häberlein, U. *J. Chem. Phys.* **1979**, *70*, 5045–5053.
- (18) Petersen, N. O.; Chan, S. I. *Biochemistry* **1977**, *16*, 2657–2667.
- (19) Bocian, D. F.; Chan, S. I. *Annu. Rev. Phys. Chem.* **1978**, *29*, 307–335.
- (20) Goetz, R.; Gompper, G.; Lipowsky, R. *Phys. Rev. Lett.* **1999**, *82*, 221–224.
- (21) Lindahl, E.; Edholm, O. *Biophys. J.* **2000**, *79*, 426–433.

dynamics manifest collective excitations of the flexible lipid molecules, rather than individual molecular motions.²² Such collective deformations of the bilayer are an essential feature of the liquid-crystalline state. The collective behavior is related to the elastic properties of aqueous lipid dispersions, as well as their self-assembly into a variety of micro- and nanostructures.

In this article, we show that by combining NMR relaxation and order parameter measurements, the results can be interpreted in terms of the material properties of fluid membrane bilayers. We provide new evidence linking the nuclear spin relaxation rates of lipid bilayers to their viscoelastic behavior on the mesoscopic scale—falling between the macroscopic and molecular dimensions—including the dependence on lipid composition, which is difficult to obtain using other methods. The rather close correspondence to previous studies of macroscopic bilayer deformations⁸ supports the physical significance of the model. The new data are discussed in terms of existing knowledge of membrane deformation, and may contribute to unifying the results of diverse biophysical techniques, encompassing a range of length and time scales. Finally, these findings give a conceptual framework for the application of nuclear spin relaxation techniques to investigations of lipid–protein interactions in relation to biomembrane functions.

Experimental Section

Synthesis of Phospholipids and Sample Preparation. The homologous series of 1,2-diperdeuterioacyl-*sn*-glycero-3-phosphocholines, that is, having perdeuterated acyl chains with lengths $n = 12, 14, 16,$ and 18 carbons, was synthesized by acylating the cadmium chloride adduct of *sn*-glycero-3-phosphocholine with the anhydride of the corresponding perdeuterated fatty acids.²³ 1,2-Diperdeuteriopalmityl-*sn*-glycero-3-phosphoethanolamine (DPPE- d_{62}) was synthesized from 1,2-diperdeuteriopalmityl-*sn*-glycero-3-phosphocholine (DPPC- d_{62}) by transphosphatidylation, using phospholipase D isolated from locally obtained Savoy cabbage (Safeway, Tucson, AZ) in the presence of ethanolamine. All lipids were purified by silica gel column chromatography, and yielded a single spot upon silica gel thin-layer chromatography using $\text{CHCl}_3/\text{MeOH}/\text{H}_2\text{O}$ (6:4:1), followed by charring with H_2SO_4 (40% in EtOH) or visualization with I_2 vapor. The phospholipids were dried under high vacuum, and random multilamellar samples were prepared for NMR spectroscopy by mixing the compounds with 50 wt % buffer containing ^2H -depleted water (Aldrich, Milwaukee, WI).

Mixtures of 1,2-diperdeuteriomyristoyl-*sn*-glycero-3-phosphocholine (DMPC- d_{54}) and cholesterol (99+%; Sigma, St. Louis, MO) were prepared by dissolving the two components in cyclohexane and lyophilization to form a dry powder, followed by hydration with 20 mM Tris buffer, pH 7.3, containing 1 mM EDTA and ^2H -depleted water.²⁴ A macroscopically oriented sample of DMPC- d_{54} /cholesterol (1:1) was made by applying the dispersion to about 20–30 glass cover slips (Corning No. 1; Corning, NY), followed by several hydration/dehydration cycles and thermal annealing to yield a final water content of ca. 70 wt %.^{24,25} Octaethyleneglycol-mono-*n*-dodecyl ether (C_{12}E_8) was procured from the Kouyoh Trading Company (Tokyo, Japan) and was used as received. DMPC- d_{54} (obtained from Avanti, Alabaster, AL)/ C_{12}E_8 /water mixtures (unbuffered, using ^2H -depleted water) were prepared by mixing and equilibrating the three components above the main lipid phase transition temperature. The samples were contained

in sealed, cutoff 8 mm test tubes, which were placed directly within the radio frequency coil of the high-power NMR probe.

Deuterium NMR Spectroscopy. Experimental ^2H NMR studies were conducted at magnetic field strengths of 7.058 T (^2H frequency of 46.13 MHz), 8.481 T (^2H frequency of 55.43 MHz), and 11.78 T (^2H frequency of 76.77 MHz). The amplifier outputs of the NMR spectrometers were used to drive external high-power amplifiers (Henry Radio, Los Angeles, CA) thereby exciting a sufficiently broad spectral bandwidth for ^2H NMR spectroscopy.²⁶ The hardware setups included home-built, thermostated NMR probes having horizontal solenoid radio frequency coils, which were capable of generating $\pi/2$ pulses as short as 1.6 μs . Transient signals from the NMR probes were acquired in quadrature, using an external preamplifier (Miteq, Hauppauge, NY) and a fast digitizer. The quadrupolar echo method was used to obtain the ^2H NMR spectra, taking care to initiate the Fourier transform at the echo maximum,²⁷ and utilizing data from both quadrature channels. Typically, an eight-step, phase-cycled quadrupolar echo pulse sequence $(\pi/2)_\phi - t_1 - (\pi/2)_{\phi \pm 90^\circ} - t_1 - \text{acquire}$ was used for spectral acquisition,²⁶ with a 2 μs $\pi/2$ pulse, a pulse pair spacing of 40 μs , a 2 μs dwell time, and a recycle time of 500 ms.

The experimental ^2H NMR spectra were deconvolved using the de-Pakeing algorithm²⁸ to obtain subspectra corresponding to the $\theta = 0^\circ$ bilayer orientation relative to the main external magnetic field. The orientational order parameters, S_{CD} , of the various C– ^2H labeled segments were evaluated both from the prominent peaks (edges or “horns”) of the experimental powder-type ^2H NMR spectra ($\theta = 90^\circ$), as well as from the de-Paked ^2H NMR spectra ($\theta = 0^\circ$), using the relation:¹²

$$|\Delta\nu_Q| = \frac{3}{2} \chi_Q |S_{\text{CD}}| |P_2(\cos \beta_{\text{DL}})| \quad (1)$$

Here $\Delta\nu_Q$ is the experimental quadrupolar splitting, $\chi_Q = 170$ kHz is the static quadrupolar coupling constant, $P_2(\cos \beta_{\text{DL}}) = (1/2)(3 \cos^2 \beta_{\text{DL}} - 1)$, where $\beta_{\text{DL}} \equiv \theta$ is the angle between the bilayer normal (D, director) and the main magnetic field direction (L, laboratory), and S_{CD} is the segmental order parameter (defined below). Spin–lattice relaxation rates, R_{1Z} , were measured by the inversion–recovery pulse sequence followed by the quadrupolar echo,¹⁷ using a 32-step modified phase cycling routine.²⁴ Typically, a 2 μs $\pi/2$ pulse, a pulse pair spacing of 30 μs , a dwell time of 7 μs , and a recycle delay of 800 ms were used for the relaxation experiments. The spin–lattice relaxation rates were obtained for each of resolved peaks in the de-Paked ^2H NMR spectra of the powder-type samples, or directly from the ^2H NMR spectra of aligned samples, using a three-parameter nonlinear regression fit to the recovery curves. All other experimental ^2H NMR methods were as described.^{24,25}

Results

Dynamical Elasticity of Membranes. Here, we consider a continuum elastic model^{15,25} for relatively slow membrane deformations, involving stress and strain of the bilayer. The analysis explains both the frequency and the angular dependencies of the R_{1Z} relaxation rates of bilayers of disaturated phospholipids in the liquid-crystalline state, as well as the observed square-law functional dependence (Figure 1). Clearly, in liquid-crystalline bilayers the phospholipid molecules are quite flexible, with numerous internal and external degrees of freedom. Assuming the relaxation is governed by relatively fast local segmental motions, then the rotational dynamics are described by a liquidlike model in terms of continuous (small-

(22) Nevzorov, A. A.; Brown, M. F. *J. Chem. Phys.* **1997**, *107*, 10288–10310.

(23) Salmon, A.; Dodd, S. W.; Williams, G. D.; Beach, J. M.; Brown, M. F. *J. Am. Chem. Soc.* **1987**, *109*, 2600–2609.

(24) Trouard, T. P.; Nevzorov, A. A.; Alam, T. M.; Job, C.; Zajicek, J.; Brown, M. F. *J. Chem. Phys.* **1999**, *110*, 8802–8818.

(25) Nevzorov, A. A.; Trouard, T. P.; Brown, M. F. *Phys. Rev. E* **1998**, *58*, 2259–2281.

(26) Bloom, M.; Davis, J. H.; Valic, M. I. *Can. J. Phys.* **1980**, *58*, 1510–1517.

(27) Davis, J. H. *Biochim. Biophys. Acta* **1983**, *737*, 117–171.

(28) Bloom, M.; Davis, J. H.; MacKay, A. L. *Chem. Phys. Lett.* **1981**, *80*, 198–202.

step) rotational diffusion,²⁹ or a jump-type model by analogy to molecular solids.^{30–32} Yet such a picture in terms of rapid trans–gauche isomerizations (which modulate the static coupling tensor)¹⁷ does not explain the ²H and ¹³C R_{1Z} rates of lipid bilayers in the fluid state as a function of frequency (magnetic field strength).²² Even in the case of ¹H and ¹³C spin–lattice (R_{1Z}) measurements at relatively high frequencies, interpretation of the data requires a significant contribution from slower lipid motions.^{13,19,22}

The slower motions of the lipids can be either collective or individual in nature.¹⁵ In essence, a lipid bilayer is a complex fluid, for which the distinguishing feature (as compared to an isotropic liquid) is the long-range ordering of its molecules. The rotational dynamics of a rigid molecule in a mean-torque potential (due to all other molecules in the bilayer) are well understood from the classical work of Pier-Luigi Nordio and co-workers.²⁹ Yet the treatment of relatively slow motions of the lipid molecules in terms of their overall rotational diffusion is somewhat different.^{15,33,34} Because of the internal flexibility of the highly entangled lipids, all the quantities in the rotational diffusion model are pre-averaged over the internal degrees of freedom; viz., the moments of inertia, the potential of mean torque, and the coupling tensor. Consideration of an “average molecule”, in terms of inertial averaging, does not readily account for the dependence of the experimental ¹H, ²H, and ¹³C R_{1Z} relaxation rates on frequency and temperature.^{13,25} Alternatively, a reduction in the number of degrees of freedom can be considered, and the bilayer modeled analogously to a molecular solid,³⁰ with different time constants for the relatively fast and slow motions.³² It is then necessary to show that such a model explains the dependence of the lipid relaxation on ordering and frequency (magnetic field strength).

By contrast, here we focus on phenomena involving distances greater than the size of the individual segments of the flexible lipids, and yet smaller than the macroscopic bilayer dimensions. In consequence, both the cohesive and the repulsive energies associated with the bilayer internal structure can exert an influence.²⁵ Comparatively slow bilayer motions involving the C–²H bonds are interpreted using models appropriate for the liquid-crystalline state of matter as a natural application. The bilayer deformations can range from long wavelength collective undulations (formulated as splay using a 2-D flexible surface model),³⁵ to shorter wavelength 3-D collective deformation modes (modeled as splay, twist, and bend),^{15,16} and finally noncollective protrusions of individual molecules^{6,36} near the short wavelength cutoff. The strongly coupled regime (2-D treatment) involves wavelength modes that are large in relation to the interbilayer separation of a multilamellar sample, for example, undulatory fluctuations giving the famous Helfrich repulsive force.^{35,37} The free membrane limit (3-D picture)

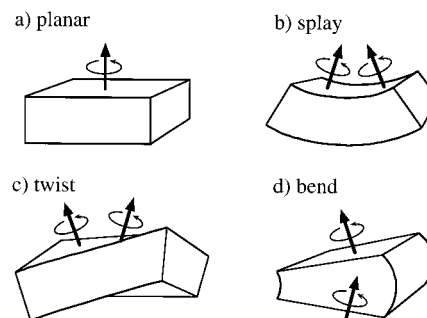


Figure 2. Illustration of possible thermal excitations of a membrane lipid bilayer in the liquid-crystalline (L_α) state within the continuum elastic approximation. (a) Planar bilayer with axial rotations about the local director; (b) splay; (c) twist; and (d) bend deformations. (For lipid bilayers, the twist and bend elastic constants are expected to be greater than for splay.)

corresponds to deformation modes approaching the bilayer thickness ($\sim 4\text{--}5$ nm) and less, yielding an $\omega^{-1/2}$ frequency dependence.¹⁶ Finally, noncollective protrusions of individual molecules⁶ can occur near the high frequency (short wavelength) cutoff and involve local motions, which provide a dynamical roughness to the bilayer.

Let us treat the former case of 3-D bilayer excitations, that is, the free membrane limit, as described by a composite membrane deformation model.²⁵ The collective thermal excitations are superimposed together with effective axial rotations of the lipids, giving a distribution of correlation times associated with quasi-coherent order fluctuations. This paradigm explains for the first time the dependencies of the R_{1Z} relaxation rates of fluid lipid bilayers on the degree of segmental ordering, on the bilayer orientation with respect to the external magnetic field, and on the nuclear resonance frequency (magnetic field strength).²⁵ A schematic depiction of such 3-D collective shape deformations of the bilayer within a continuum approximation is provided in Figure 2. The order fluctuations are modeled as unconstrained splay, twist, and bend excitations. We also assume that a slowly fluctuating torque acts upon the chains, yielding effective axial rotations of the lipids about a local director.²⁵ A key aspect is that the spectral density is distributed broadly in frequency, and for a given value of the S_{CD} order parameter, the segmental R_{1Z} value is related to the dynamical “softness” of the bilayer. A larger R_{1Z} for the same value of S_{CD} corresponds to a shift of the spectral density from higher to lower frequencies—in other words, a softer bilayer, and vice versa. However, an alternative is that discrete rotational modes of the flexible lipid molecules largely account for the NMR relaxation rates of fluid bilayers in the megahertz range.^{33,34} Thus, it is desirable to further test the physical significance of the composite membrane deformation model by conducting additional investigations.

Segmental Order Parameters—Equilibrium Structure. For the ²H nucleus with spin $I = 1$, the solid-state NMR spectra comprise two transitions, whose separation in frequency units is called the quadrupolar splitting. (According to quantum mechanics, coupling of the ²H nuclear quadrupole moment with the electric field gradient (EFG) of the C–²H bond gives an orientation-dependent perturbation of the magnetic Zeeman Hamiltonian.) Figure 3 shows ²H NMR spectra of a multilamellar dispersion of a representative phospholipid in excess water, viz., 1,2-diperdeuteriopalmitoyl-*sn*-glycero-3-phosphoethanolamine, DPPE- d_{62} , having perdeuterated acyl chains, in the liquid-crystalline (L_α) state. Figure 3a indicates the powder-

(29) Nordio, P. L.; Segre, U. In *The Molecular Physics of Liquid Crystals*; Luckhurst, G. R., Gray, G. W., Eds.; Academic Press: New York, 1979; pp 411–426.

(30) Torchia, D. A.; Szabo, A. J. *Magn. Reson.* **1982**, *49*, 107–121.

(31) Siminovich, D. J.; Ruocco, M. J.; Olejniczak, E. T.; Das Gupta, S. K.; Griffin, R. G. *Chem. Phys. Lett.* **1985**, *119*, 251–255.

(32) Speyer, J. B.; Weber, R. T.; Das Gupta, S. K.; Griffin, R. G. *Biochemistry* **1989**, *28*, 9569–9574.

(33) Rommel, E.; Noack, F.; Meier, P.; Kothe, G. *J. Phys. Chem.* **1988**, *92*, 2981–2987.

(34) Halle, B. *J. Phys. Chem.* **1991**, *95*, 6724–6733.

(35) Helfrich, W.; Servuss, R.-M. *Nuovo Cimento* **1984**, *3*, 137–151.

(36) McIntosh, T. J.; Advani, S.; Burton, R. E.; Zhelev, D. V.; Needham, D.; Simon, S. A. *Biochemistry* **1995**, *34*, 8520–8532.

(37) Podgornik, R.; Parsegian, V. A. *Langmuir* **1992**, *8*, 557–562.

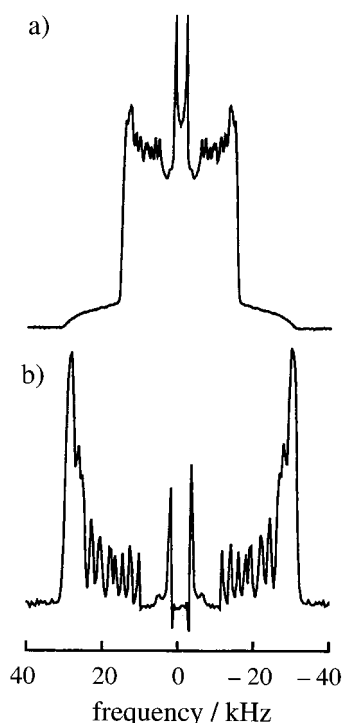


Figure 3. Representative ^2H NMR spectra of 1,2-diperdeuteriopalmityl-*sn*-glycero-3-phosphoethanolamine (DPPE- d_{62}) in the fluid (L_α) phase. The sample contained 50 wt % H_2O (20 mM MOPS buffer, 1 mM EDTA, pH 7.1) at $T = 69^\circ\text{C}$, and the ^2H NMR spectra were acquired at 46.1 MHz (7.06 T). (a) Experimental ^2H NMR spectrum of randomly oriented multilamellar dispersion; and (b) corresponding de-Paked ^2H NMR spectrum due to $\theta = 0^\circ$ orientation. A distribution of quadrupolar couplings is evident, which is related to the profile of segmental order parameters as a function of acyl position.

type ^2H NMR spectrum of the randomly oriented, multilamellar dispersion. The prominent edges or “horns” stem from the $\theta = 90^\circ$ bilayer orientation (normal to membrane surface perpendicular to magnetic field), and the weaker shoulders with twice the quadrupolar splitting manifest the $\theta = 0^\circ$ alignment. Various residual splittings are evident, which originate from the motionally inequivalent lipid segments. Figure 3b shows the corresponding “de-Paked” ^2H NMR spectrum, which is obtained from the spectrum in part a (by numerical deconvolution) and is due to the $\theta = 0^\circ$ orientation (membrane normal parallel to magnetic field).²⁸ An obvious improvement in resolution is found, as the de-Paked ^2H NMR spectrum represents a specific bilayer orientation, for which the quadrupolar splittings are spread out to the maximum extent possible.¹²

The residual quadrupolar splittings are directly related to the orientational order parameters of the flexible lipid molecules in the fluid, lamellar (L_α) state. They characterize the angular amplitudes of the motions of the various $\text{C}-^2\text{H}$ labeled segments, and manifest the dynamical structure of the bilayer.^{4,12} The order parameters are defined as

$$S_{\text{CD}}^{(i)} \equiv \frac{1}{2} \langle 3 \cos^2 \beta_{\text{PD}}^{(i)} - 1 \rangle \quad (2)$$

where $\beta_{\text{PD}}^{(i)}$ is the angle between the i th $\text{C}-^2\text{H}$ bond (P, principal symmetry axis of the EFG) and the macroscopic bilayer normal, known as the director (D). (The angular brackets pertain to motional averaging over the characteristic time scale associated with the ^2H NMR transitions, which for multilamellar

lipid dispersions is $(2\pi \times (9/8)\chi_Q)^{-1} \approx 10^{-6}$ s.) The segmental order parameters provide knowledge of the projected length of the acyl chains and the associated bilayer hydrocarbon thickness, the aqueous interfacial area occupied per lipid molecule, and the response of the bilayer to external forces.³⁸ One should note that knowledge of position is not obtained directly, and must be inferred through application of an appropriate statistical model.^{23,38–40}

Nuclear Spin Relaxation—Structural Dynamics. Additionally, dynamical properties of the flexible phospholipids are manifested by the corresponding nuclear spin relaxation rates. These describe the types, rates, and amplitudes of the various motions of the phospholipid segments that give rise to averaging of their coupling tensors.¹² Fluctuations of the molecule-fixed coupling tensor relative to the laboratory frame yield a time-dependent perturbation of the Zeeman Hamiltonian, which induces transitions among the various nuclear energy levels, leading to relaxation to the equilibrium Boltzmann distribution. Simply put, the nuclear spin relaxation rates characterize the fluctuations due to segmental, molecular, and collective motions of the lipids in the megahertz range (spectral densities of motion or power spectra). Such relaxation measurements can detect both local motions and the larger-scale dynamical behavior of membrane phospholipids. In consequence, solid-state NMR spectroscopy provides a unique window into time-dependent properties in terms of fluctuations of the coupling interactions about their equilibrium or average values.

The NMR relaxation rates (or spectral densities) allow one to disentangle the motions giving rise to the segmental order parameter S_{CD} . The nuclear spin relaxation corresponds to the fluctuating part of the interaction (in the present case the electric quadrupolar coupling).^{12,13,41} The relaxation manifests the strength of the $\text{C}-^2\text{H}$ bond fluctuations as a function of frequency, and thus are associated with the lipid motions, for example, the “softness” of the membrane bilayer. Generally speaking, the relaxation rates depend on the mean-squared amplitudes of the fluctuations of the $\text{C}-^2\text{H}$ labeled molecules, and the correlation times for the associated lipid reorientational motions near the nuclear Larmor frequency (megahertz range). Rapid local motions of the $\text{C}-^2\text{H}$ bonds can occur due to trans-gauche isomerizations and out of plane displacements (protrusions) of the lipid groups, which change the $\text{C}-^2\text{H}$ bond orientations with respect to the membrane normal and modulate the *static* EFG tensor relative to its average value. Likewise, slower motions of the membrane lipids can occur, which lead to further modulation of the remaining *residual* EFG tensor, and also produce a change in orientation of the $\text{C}-^2\text{H}$ segments. The comparatively slow lipid motions can be due to rotations of the lipid molecules within the membrane, that is, molecular motions,^{15,18,33,34} and/or collective thermal excitations of the bilayer.^{15,42–44} For a composite membrane deformation model (cf. Appendix), the collective motions are superimposed together

(38) Petrache, H. I.; Dodd, S. W.; Brown, M. F. *Biophys. J.* **2000**, *79*, 3172–3192.

(39) Seelig, J.; Seelig, A. *Q. Rev. Biophys.* **1980**, *13*, 19–61.

(40) Jansson, M.; Thurmond, R. L.; Barry, J. A.; Brown, M. F. *J. Phys. Chem.* **1992**, *96*, 9532–9544.

(41) Long, J. R.; Ebelhauser, R.; Griffin, R. G. *J. Phys. Chem. A* **1997**, *101*, 988–994.

(42) Brown, M. F.; Davis, J. H. *Chem. Phys. Lett.* **1981**, *79*, 431–435.

(43) Pace, R. J.; Chan, S. I. *J. Chem. Phys.* **1982**, *76*, 4228–4240.

(44) Weisz, K.; Gröbner, G.; Mayer, C.; Stohrer, J.; Kothe, G. *Biochemistry* **1992**, *31*, 1100–1112.

with effective molecular rotations and faster trans–gauche acyl isomerizations,²⁵ leading to the observed nuclear spin relaxation.

Using various pulsed NMR techniques, the nuclear spin relaxation rates of the resolved ²H NMR splittings can be measured as pioneered by Regitze Vold and co-workers.⁴⁵ The spin–lattice (longitudinal) relaxation rate R_{1Z} is due to motions of the individual C–H bonds (the EFG) relative to the laboratory frame, as defined by the main external magnetic field. It is given to second-order in the perturbing Hamiltonian by^{12,45–47}

$$R_{1Z} = \frac{3}{4} \pi^2 \chi_Q^2 [J_1(\omega_D) + 4J_2(2\omega_D)] \quad (3)$$

where ω_D is the deuteron resonance (Larmor) frequency. (In terms of the Bloch–Wangsness–Redfield theory,⁴⁶ R_{1Z} describes the coupling of the ²H nuclear spins to the lattice (surroundings) within the weak collision regime.) The symbols $J_m(\omega)$ indicate the (irreducible) spectral densities of motion:

$$J_m(\omega) = \int G_m(t) \exp(-i\omega t) dt \quad (4)$$

in which ω is the angular frequency, and t is time. In the above expression, $G_m(t)$ denotes the temporal autocorrelation functions (rank-2) of the perturbing Hamiltonian ($m = 1, 2$). Equation 3 shows how relaxation rate measurements are connected to the membrane dynamics in terms of the spectral densities (power spectra) of the lipid motions that produce averaging of the coupling tensor.

Spectroscopic Observables—Model-Free Aspects. Clearly, the NMR observables can involve a hierarchy of motions, which contribute to the dynamical roughness of the bilayer. Taken together, the values of $|S_{CD}^{(i)}|$ and $R_{1Z}^{(i)}$, that is, as a function of the lipid acyl chain position (i), provide a rich source of structural and dynamical information in the case of membrane lipids.¹² What can be said in terms of a model-free interpretation? It is well established that in the fluid state a profile of the $|S_{CD}^{(i)}|$ and $R_{1Z}^{(i)}$ values is observed, with the largest values at the beginning of the chain, closest to the polar headgroups, followed by a progressive decrease toward the bilayer center (Figure 1).¹⁷ In brief, one has an order function $|S_{CD}^{(i)}|$ related to the mean-squared amplitudes of the various acyl segments (index i). By contrast, the segmental relaxation function, for example, $R_{1Z}^{(i)}$, involves both the mean-squared amplitudes and the rates of the motions (reduced spectral densities),¹² that is, the order parameters $S_{CD}^{(i)}$ as well as the associated correlation times, where the latter may encompass a distribution of values. Further, some conclusions of a general nature can be drawn that are relatively independent of the detailed motional model used for analysis of the experimental NMR data. For multilamellar lipid dispersions, as well as small lipid vesicles, the relaxation rates are averaged over all bilayer orientations on the time scale of the nuclear spin relaxation (milliseconds).⁴² In the limit of orientational averaging of the relaxation, the mean-squared amplitude of the segmental motions is proportional to $(1 - S_{CD}^2)$, where

the index i is suppressed. Conservation of energy requires that the mean-squared interaction strength (corresponding to the area under the spectral density function) is reduced in ordered systems, such as lipid bilayers, as compared to the isotropic case ($S_{CD} = 0$). It follows that the relaxation is less efficient, since not all of the angular-dependent interaction is fluctuating.¹⁵

Let us next consider the case that there are multiple motions. As noted above, fast segmental motions can partially average the quadrupolar coupling, as described by a fast order parameter $S_f^{(2)}$. (Here the superscript indicates that the coupling interaction is rank-2.) Slower lipid motions (of larger overall amplitude) then lead to further averaging, as given by a slow order parameter $S_s^{(2)}$. The additional averaging due to the slower motions yields the observed order parameter S_{CD} , given by the product $S_{CD} = S_f^{(2)} \tilde{S}_{int}^{(2)} S_s^{(2)}$ (assuming uncorrelated motions). Here, $\tilde{S}_{int}^{(2)}$ is a geometric factor²⁵ for the internal frame that relates the comparatively fast and slow motions, and describes the orientation of the local director field. In analogy to the fast motions, the mean-squared amplitude of the *slow* motions (i.e., the area of the spectral density function) is proportional to $S_f^{(2)2}(1 - S_s^{(2)2})$. Provided the relatively slow motions are the same along the acyl chain (index i), the observed order parameters $S_{CD}^{(i)}$ scale with the fast segmental order parameters $S_f^{(2,i)}$, resulting in a square-law dependence of the $R_{1Z}^{(i)}$ rates on $S_{CD}^{(i)}$.

The approximately quadratic *increase* in the $R_{1Z}^{(i)}$ rates, viz., the motional spectral density, as $|S_{CD}^{(i)}|$ increases toward the chain beginning (Figure 1) is contrary to what is expected for segmental fast motions, which modulate the *static* coupling tensor. On the other hand, a square-law dependence of the two spectroscopic observables is a hallmark of relatively slow motions that modulate the local bilayer structure set up by more rapid acyl segmental motions, that is, which modulate the *residual* coupling tensors along the chains. Hence, relatively slow motions provide the dominant R_{1Z} contribution in fluid lipid bilayers. The observed square-law relation is independent of any motional model and can shed new light on the structural dynamics of bilayer membranes. By comparing the $R_{1Z}^{(i)}$ values for the same value of $S_{CD}^{(i)}$, for example, in terms of a square-law functional dependence, one is able to gain an idea of the fluctuating part of the interaction (related to the bilayer softness).

Homologous Series of Phosphatidylcholines—Influences of Acyl Length on Bilayer Flexibility. In one set of experiments, a homologous series of saturated phosphatidylcholines was investigated in the liquid-crystalline (L_α) phase with excess water (50 wt %), having perdeuterated acyl chains ranging in length from $n = 12$ to 18 carbons. The use of acyl chain-perdeuterated phospholipids is advantageous in that one is able to observe the behavior of the entire hydrocarbon region of the bilayer simultaneously.^{24,48} Randomly oriented, multilamellar dispersions were employed, in which the prominent peaks in the ²H NMR spectra correspond to the $\theta = 90^\circ$ bilayer orientation; that is, the director axis (normal to the bilayer surface) was perpendicular to the main magnetic field.¹² In Figure 4, the observed spin–lattice relaxation rate, $R_{1Z}^{(i)}$, for each of the resolved quadrupolar splittings is plotted against the corresponding squared segmental order parameter $|S_{CD}^{(i)}|$, at a series of different temperatures, for the homologous series of 1,2-

(45) Vold, R. R. In *Nuclear Magnetic Resonance Probes of Molecular Dynamics*; Tycko, R., Ed.; Kluwer Academic Publishers: Dordrecht, 1994; pp 27–112.

(46) Slichter, C. P. *Principles of Magnetic Resonance*, 3rd ed.; Springer-Verlag: Heidelberg, 1990.

(47) Bloom, M.; Morrison, C.; Sternin, E.; Thewalt, J. L. In *Pulsed Magnetic Resonance: NMR, ESR, Optics*; Baggeley, D. M. S., Ed.; Clarendon Press: Oxford, 1992; pp 274–316.

(48) Morrison, C.; Bloom, M. *J. Chem. Phys.* **1994**, *101*, 749–763.

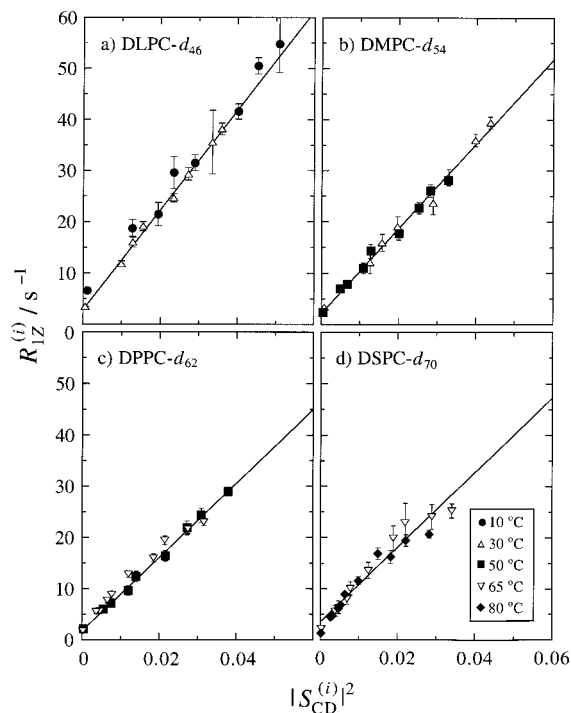


Figure 4. Square-law functional dependence of spin–lattice relaxation rates $R_{1Z}^{(i)}$ and order parameters $|S_{CD}^{(i)}|^2$ along the acyl chains (index i) for homologous series of 1,2-diperdeuterioacyl-*sn*-glycero-3-phosphocholines in the fluid (L_α) phase. Data are for randomly oriented multilamellar dispersions (powder-type samples), containing 50 wt % H₂O (67 mM phosphate buffer, pH 7.0) at 55.4 MHz (8.48 T) and temperatures of $T = 10, 30, 50, 65,$ and 80 °C (●, △, ■, ▽, ◆, respectively). Results are shown for (a) DLPC- d_{46} ; (b) DMPC- d_{54} ; (c) DPPC- d_{62} ; and (d) DSPC- d_{70} , with acyl lengths of $n = 12, 14, 16,$ and 18 carbons, respectively. Note that increasing the acyl length leads to a small reduction of the square-law slope and that the data at different temperatures are nearly superimposable (cf. text).

diacyl-*sn*-glycero-3-phosphocholines with perdeuterated acyl chains. As can be seen, a square-law functional dependence of the $R_{1Z}^{(i)}$ rates on the order parameters $|S_{CD}^{(i)}|^2$ along the chains is found for the entire homologous series to a reasonably good approximation, indicating a model-free correlation of the spectroscopic observables, with a small ordinate intercept.

Moreover, comparison of the results in Figure 4a–d indicates that there is rather little influence of the acyl length on the square-law correlation of $R_{1Z}^{(i)}$ and $|S_{CD}^{(i)}|^2$ for the homologous series of PCs. A small reduction in the slopes ($\sim 25\%$) and similar ordinate intercepts is evident. Analysis of the order profiles³⁸ reveals that the major effect of the lipid acyl chain length is to increase the bilayer hydrocarbon thickness, whereas the interfacial area per molecule shows only a slight contraction (due to increased attractive van der Waals forces). The lack of an appreciable dependence of the data in Figure 5 on the bilayer thickness is consistent with a composite 3-D membrane deformation model (cf. Appendix), in which the fluctuation wavelengths are on the order of the bilayer thickness and even less. Assuming the splay elastic constant K_{11} (N) is related to the splay modulus κ (also known as the bending rigidity) (J) and the bilayer thickness t by $K_{11} = \kappa/t$, the results imply that κ increases with the bilayer thickness t for the homologous phosphatidylcholines. This is in accord with physical intuition, as it costs more energy to deform a thicker bilayer. The above conclusion is also consistent with the macroscopic elastic

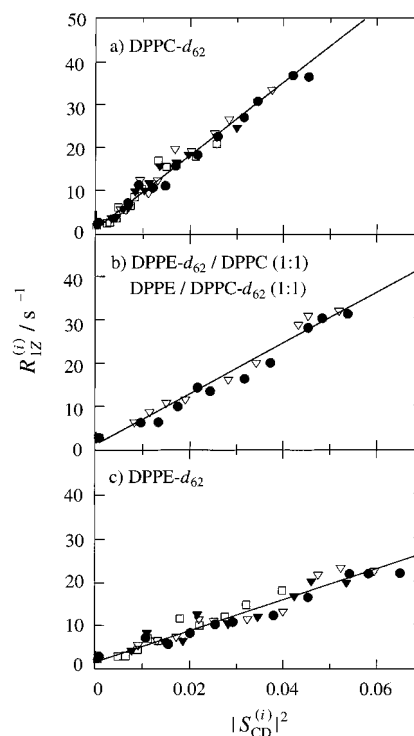


Figure 5. Square-law functional dependence of $R_{1Z}^{(i)}$ and $|S_{CD}^{(i)}|^2$ for phospholipid bilayers in the L_α phase, showing influence of phosphoethanolamine headgroups (interfacial area per molecule). Data are for unoriented multilamellar lipid dispersions (powder-type samples), containing 50 wt % H₂O (20 mM MOPS buffer, 1 mM EDTA, pH 7.1) at 46.1 MHz (7.06 T). Results are shown for (a) DPPC- d_{62} at $T = 42, 50, 65,$ and 80 °C (●, ▽, ▼, □, respectively); (b) DPPE- d_{62} /DPPC (1:1) and DPPE/DPPC- d_{62} (1:1) at 65 °C (▽ and ●, respectively); and (c) DPPE- d_{62} at $T = 60, 65, 69,$ and 80 °C (●, ▽, ▼, □, respectively). A progressive decrease in the slope of the square-law plots due to the presence of DPPE- d_{62} is seen as compared to DPPC- d_{62} in the liquid-crystalline state (cf. text).

properties of giant PC vesicles investigated by shape fluctuations and micropipet deformation, which indicate that κ increases with the acyl length for saturated PCs.^{49,50}

Phosphatidylcholine Series—Thermal Effects on NMR Observables. The influences of temperature can also help to further understand the types of motions governing the relaxation in the case of flaccid (tensionless) membranes. According to Figure 4, rather little influence of temperature is observed on the square-law plots of $R_{1Z}^{(i)}$ against $|S_{CD}^{(i)}|^2$. In fact, the entire data set in Figure 4a–d can be superimposed in terms of a nearly universal flexibility plot for the homologous series of PCs, indicating that both the temperature and the acyl length dependencies of the relatively slow motions causing the relaxation are small. The observation that a broad range of ²H NMR spectral and relaxation data, involving four different saturated PCs over a range of temperatures in the liquid-crystalline state, can be unified in terms of a simple square law is striking.

Now the conventional interpretation of such NMR relaxation data involves the Arrhenius law, in which the thermal behavior is due to the *rate* of motions, for example, as manifested by the reduced spectral densities and associated correlation times. Yet an alternative¹⁵ is that the intrinsic temperature dependence

(49) Fernandez-Puente, L.; Bivas, I.; Mitov, M. D.; Méléard, P. *Europhys. Lett.* **1994**, *28*, 181–186.

(50) Rawicz, W.; Olbrich, K. C.; McIntosh, T.; Needham, D.; Evans, E. *Biophys. J.* **2000**, *79*, 328–339.

of the comparatively slow motions is weak and that temperature mainly influences the mean-squared amplitudes due to faster motions, such as trans–gauche isomerizations. Consequently, the relaxation is mainly affected by temperature through the mean-squared amplitudes of the fast *local* motions, that is, in terms of the Boltzmann law, rather than the reduced spectral densities which describe the relatively *slow* motions.¹⁵ The absence of a strong temperature dependence of the square-law slopes (Figure 4) implies the modes governing the relaxation²² are not strongly thermally activated—a possible hallmark of collective fluctuations involving the hydrocarbon region of membrane bilayers. The above inference agrees with studies of thermal shape fluctuations of giant lipid vesicles in the L_α state employing video microscopy. Such studies reveal that the variation of the splay elastic modulus κ with temperature is rather small, except in the immediate vicinity of the phase transition temperature T_m .^{49,51} The weak temperature dependence is consistent with the idea that the effective axial rotations are not due to individual molecules, but rather are a property of the phase stemming from slowly fluctuating torques that are themselves not strongly temperature dependent.

Estimation of Material Constants. For DMPC- d_{54} in the L_α phase, we have conducted a more detailed study of the angular anisotropy and frequency dependence of the R_{1Z} rates in the megahertz range in terms of a composite membrane deformation model, that is, to linear order in the local director fluctuations.²⁵ The analysis enables one to estimate the individual contributions (collective, molecular, and cross-term) to the spectral densities due to comparatively slow motions (cf. Appendix). Application to the experimental R_{1Z} rates of DMPC- d_{54} in the L_α phase²⁵ results in a viscoelastic constant of $D = 3k_B T \sqrt{\eta/5\pi} \sqrt{2K^3(S_s^{(2)\text{col}})^2} = 1.0 \times 10^{-5} \text{ s}^{1/2}$. Here, K is the (single) elastic constant for the bilayer deformations, η is the corresponding viscosity coefficient, and the other symbols have their conventional definitions. As the present NMR relaxation approach is a dynamical method, it does not yield the deformation energy directly, but rather involves the effective membrane viscosity⁵² together with the mean-squared amplitudes as described by the collective slow order parameter $S_s^{(2)\text{col}}$. The experimental value⁵⁰ of the splay modulus (so-called bending rigidity) $\kappa = K_{11}t = 14 k_B T$, obtained from micromechanical measurements, implies a fairly soft (semi-flexible) bilayer. (Note that κ may depend on the length scale.) Using the value of κ for the DMPC bilayer⁵⁰ as a reference, we can then estimate κ for the other members of the homologous series of PCs from the relation $(\kappa/t)' = (m/m')^{2/3}(\kappa/t)$, where the prime denotes the lipid of interest, and m is the slope of the corresponding square-law plot. For acyl lengths ranging from C_{12} to C_{18} , assuming an increase in the bilayer thickness of 1.2 nm at 65 °C³⁸ we obtain a 60% increase in κ , in excellent agreement with micromechanical deformation⁵⁰ and thermal shape fluctuation⁴⁹ studies of giant PC vesicles.⁵³ Additionally, one is able to calculate the area elastic constant K_a from continuum mechan-

ics^{20,50} with use of the relation $\kappa = K_a t^2/48$, giving for DMPC- $d_{54} \approx 210 \text{ mJ m}^{-2}$, in the range for fluid bilayers.⁵

An heuristic calculation then uses the experimental value of κ for the DMPC bilayer⁵⁰ as a reference to calculate the slow order parameter, and thereby obtain an estimate of the amplitude of the relatively slow order fluctuations (cf. Appendix).^{22,25} Here, we assume an effective membrane viscosity of $\eta \approx 1 \text{ P}$,⁵² corresponding to our more detailed relaxation analysis of the DMPC- d_{54} bilayer.²⁵ We obtain that $S_s^{(2)\text{col}} \approx 0.5\text{--}0.6$, which is consistent with previous estimates using a molecular model.¹² The collective slow order parameter $S_s^{(2)\text{col}}$ for DMPC- d_{54} can then be used to calculate the rms angular amplitude (β_{ND}) of the comparatively slow order fluctuations, using $|S_s^{(2)\text{col}}| \approx 1 - (3/2)\langle\beta_{\text{ND}}^2\rangle$, giving $\langle\beta_{\text{ND}}^2\rangle^{1/2} \approx 30^\circ$, an appreciable value. In the single elastic constant approximation $1/\tau_q = Kq^2/\eta$, where q is the wavenumber, and since the most important fluctuations for nuclear spin relaxation are those where $\omega_0\tau_q \approx 1$, the corresponding wavelength is $\lambda = 2\pi/q = 2\pi(K/\eta\omega_0)^{1/2}$. Use of the above values of K and η together with $\omega_0/2\pi = 46.1\text{--}76.8 \text{ MHz}$ gives $\tau_q \approx 2\text{--}3 \text{ ns}$ with $\lambda \approx 4 \text{ nm}$, on the order of the bilayer thickness. In turn, the angular amplitude $\langle\beta_{\text{ND}}^2\rangle^{1/2}$ of the relatively slow order fluctuations allows one to estimate the cutoff frequency in q -space, or equivalently the wavelength cutoff for the collective motions. For such a quasi-nematic treatment,²² the relation $\langle\beta_{\text{ND}}^2\rangle = k_B T q_c / \pi^2 K$ gives a relatively short wavelength cutoff of $\lambda_c = 2\pi/q_c \approx 3 \text{ \AA}$. This is substantially less than the bilayer thickness and is close to the acyl cross-sectional diameter in the fluid phase,^{12,38} in the range expected for molecular protrusions from the bilayer surface. The corresponding high-frequency cutoff is estimated as $\omega_c/2\pi = 2\pi K/\eta\lambda_c^2 \approx 10 \text{ GHz}$, well above the NMR observation frequency (megahertz range), justifying a posteriori its neglect in the reduced spectral densities. Application of a quasi-nematic picture for collective bilayer fluctuations thus supports our contention that q -modes of appreciable amplitude govern the relaxation within the megahertz regime, having correlation times in the nanosecond range, and component wavelengths ranging down to the bilayer thickness and even less.

Influences of Phosphatidylethanolamine on Membrane Elasticity. We have also studied bilayers containing phosphatidylethanolamine (PE) to investigate the role of the polar headgroups. Figure 5 shows results for multilamellar dispersions containing DPPE- d_{62} and DPPC- d_{62} , encompassing a series of different temperatures in the fluid (L_α) phase. Here, the segmental $R_{1Z}^{(i)}$ rates and the $|S_{\text{CD}}^{(i)}|$ values in the L_α phase depend on both the lipid composition and the temperature, in addition to the acyl segment position. The data in Figure 5 imply that for both DPPE- d_{62} as well as DPPC- d_{62} the two observables are correlated over the entire temperature range by a square-law functional dependence. Yet a completely universal behavior is not observed for the entire series of glycerophospholipids investigated, that is, considering both PE and PC headgroups. Rather, as compared to DPPC- d_{62} alone, Figure 5a, with increasing mole fraction of DPPE- d_{62} there is a systematic decrease in $R_{1Z}^{(i)}$ for a given value of the order parameter $|S_{\text{CD}}^{(i)}|$, cf. Figure 5b and c, which is model-free. The rather obvious reduction in the slope of the square-law plots of $R_{1Z}^{(i)}$ versus $|S_{\text{CD}}^{(i)}|^2$, with similar ordinate intercepts, is independent of any motional model. In terms of a composite deformation model, the influences of the PE headgroups can involve the fast order

(51) Méléard, P.; Gerbaud, C.; Pott, T.; Fernandez-Puente, L.; Bivas, I.; Mitov, M. D.; Dufourcq, J.; Botharel, P. *Biophys. J.* **1997**, *72*, 2616–2629.

(52) Gennis, R. B. *Biomembranes: Molecular Structure and Function*; Springer-Verlag: New York, 1989.

(53) The estimated material constants differ slightly from those in a preliminary report due to use of the experimental value of κ as a reference, see: Brown, M. F.; Thurmond, R. L.; Dodd, S. W.; Otten, D.; Beyer, K. *Phys. Rev. E* **2001**, *64*, 10901-1–10901-4.

parameter $S_f^{(2)}$, the elastic constant K , and the effective axial diffusion rate. Previous work has shown that in the L_α phase the observed $|S_{CD}^{(i)}|$ order profiles increase in absolute magnitude for PE versus PC; that is, there is an increase in bilayer thickness.^{38,54} Within this framework it is plausible that the fast and slow order parameters scale proportionally. Consequently, the model implies that the PE headgroups influence the viscoelastic behavior, possibly together with the rate of effective lipid axial rotations. As described above, the experimental value of κ for the DMPC bilayer⁵⁰ can be adopted as a reference. Taking a value of $t \approx 4$ nm³⁸ then gives $\kappa \approx 31 k_B T$ and $K_a \approx 400$ mJ m⁻² for the DPPE- d_{62} bilayer. Thus, the presence of PE headgroups leads to an appreciable stiffening of the lipid membrane as compared to PC.

Bilayer Additives—Opposite Effects of Detergents and Cholesterol. The biophysical relevance of these findings is further supported by our investigations of the effects of various solutes, encompassing a nonionic cosurfactant, $C_{12}E_8$, and cholesterol. Previous macroscopic studies of membrane deformation⁸ have shown opposite influences of cholesterol and surfactants such as $C_{12}E_8$ on the bilayer flexibility, for example, as observed via static membrane deformation^{5,36,50} or thermally induced bilayer undulations.^{8,51} Addition of a cosurfactant yields a softening of the bilayer, whereas cholesterol is associated with a greater bilayer rigidity. To establish the correspondence to investigations of bilayers treated as a continuum material, we examined DMPC- d_{54} containing the nonionic surfactant $C_{12}E_8$, which is of the alkyl poly[ethylene oxide] series, as well as cholesterol (Figure 6). As shown in Figure 6a, the presence of $C_{12}E_8$ in the DMPC- d_{54} bilayer (1:2 molar ratio) yields an increase in R_{1Z} for a given value of S_{CD} ; viz., there is an increase in the slope of the square-law plots versus the DMPC- d_{54} bilayer alone, with little change in intercept. Although both R_{1Z} and S_{CD} are altered by the presence of detergent in the bilayer, the data are described by a simple square-law functional dependence, to a reasonable approximation. The substantial increase in the slope of the square-law plot versus DMPC- d_{54} alone is interpreted as due to a softening of the bilayer by the presence of a cosurfactant, possibly together with a decrease in the effective axial diffusion rate arising from increased chain entanglement. The estimated value of κ is $\sim 7 k_B T$, and the corresponding value of K_a is ~ 150 mJ m⁻², both evincing a substantial decrease versus the reference DMPC- d_{54} bilayer due to the presence of the nonionic surfactant $C_{12}E_8$.

By contrast, Figure 6b shows that inclusion of cholesterol in the DMPC- d_{54} bilayer (1:1 molar ratio; liquid-ordered phase) leads to effects that are qualitatively similar to those of PE headgroups (vide supra), albeit substantially greater.²⁴ For a given value of S_{CD} , there is a substantial decrease in the R_{1Z} relaxation rate for the case of DMPC- d_{54} /cholesterol (1:1) bilayers versus DMPC- d_{54} alone. As can be seen in Figure 6b, the square-law plot for the liquid-ordered phase of DMPC- d_{54} /cholesterol (1:1) bilayers indicates an appreciable reduction of the slope as compared to DMPC- d_{54} in the L_α phase, with a similar intercept. We attribute this to a stiffer bilayer, leading to a smaller contribution from collective bilayer motions, in agreement with studies of macroscopic bilayer fluctuations.⁵¹ Application of a composite membrane deformation model (cf.

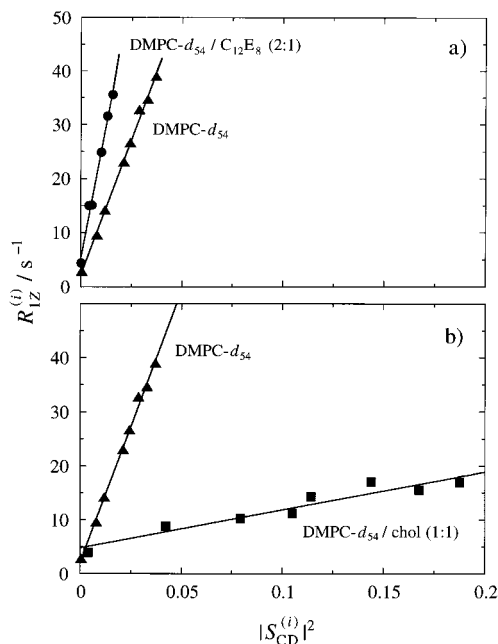


Figure 6. Square-law functional dependence of $R_{1Z}^{(i)}$ and $|S_{CD}^{(i)}|$ for DMPC- d_{54} , showing influence of a nonionic cosurfactant, $C_{12}E_8$, in the L_α phase and cholesterol in the liquid-ordered phase. The results are for bilayers aligned at $\theta = 90^\circ$, containing excess H_2O at 46.1 MHz (7.06 T). (a) Square-law plot for DMPC- d_{54} / $C_{12}E_8$ (2:1) system (●) containing 95 wt % H_2O (aligned at $\theta = 90^\circ$ by the magnetic field) at $T = 42^\circ C$, as compared to DMPC- d_{54} (▲) containing ca. 70 wt % H_2O (20 mM Tris buffer, 1 mM EDTA, pH 7.3; aligned mechanically at $\theta = 90^\circ$ on planar glass substrates) in the L_α phase at $T = 40^\circ C$. (b) Square-law plot for DMPC- d_{54} /cholesterol (1:1) system (■) containing ca. 70 wt % H_2O (20 mM Tris buffer, 1 mM EDTA, pH 7.3; mechanically aligned at $\theta = 90^\circ$) in the liquid-ordered phase, as compared to DMPC- d_{54} (▲) containing ca. 70 wt % H_2O (20 mM Tris buffer, 1 mM EDTA, pH 7.3, mechanically aligned) in the L_α phase at $T = 40^\circ C$. Note the opposite effects of the nonionic surfactant and cholesterol on the square-law plots; $C_{12}E_8$ increases the slope, whereas cholesterol yields a pronounced decrease (cf. text).

Appendix) implies there is an increase in the viscoelastic constant for bilayer deformations, possibly accompanied by a larger rate of effective axial diffusion of the phospholipids.²⁴ The NMR relaxation data yield a viscoelastic constant of $D = 4.9 \times 10^{-7} s^{1/2}$ for the DMPC- d_{54} /cholesterol (1:1) bilayer,²⁴ which together with the reference value²⁵ for DMPC- d_{54} gives $K_{DMPC/chol} = (D_{DMPC}/D_{DMPC/chol})^{2/3} K_{DMPC} \approx 9.3 \times 10^{-11}$ N. This indicates about an 8-fold increase in the elastic constant K due to incorporation of cholesterol in the DMPC bilayer, that is, in the liquid-ordered phase.²⁴ Assuming $t \approx 5$ nm gives $\kappa \approx 110 k_B T$ for the bending rigidity, with a correspondingly large increase in the area elastic modulus ($K_a \approx 900$ mJ m⁻²). The above results for cholesterol are opposite of the influences of $C_{12}E_8$, and thus correspond to macroscopic studies of membrane deformations.⁸

Discussion

In deuterium (2H) NMR spectroscopy of lipid bilayers in the fluid (L_α) phase, the experimental quantities are the order parameters (S_{CD}) of the various inequivalent segments of the flexible molecules, and the corresponding spin–lattice (Zeeman) relaxation rates (R_{1Z}). By combining NMR spectral measurements and relaxation studies, we have obtained greater knowledge than with either methodology alone. Here, we have shown how the segmental R_{1Z} relaxation rates of liquid-crystalline bilayers together with the segmental order parameters S_{CD} imply

(54) Thurmond, R. L.; Dodd, S. W.; Brown, M. F. *Biophys. J.* **1991**, *59*, 108–113.

collective properties of the membrane lipids.¹⁵ Our results indicate that *combined* R_{1Z} and S_{CD} studies of phospholipids can be used as a simple membrane elastometer on the mesoscopic length scale of the bilayer thickness and less. Because the present ^2H NMR measurements are inherently accurate and reproducible, one can identify systems that can be further investigated using complementary biophysical techniques.^{5,8,36,49–51,55–58} An important aim is to develop a more comprehensive and realistic picture of soft states of matter, such as lipid bilayers, which can be further refined by molecular dynamics simulations.^{20,21,59–62} By considering simplified treatments in mathematical closed form, the predominant types of motions in fluid membranes can be identified. Extension in terms of molecularly specific computer models^{21,59–64} is then possible.

Despite many earlier investigations, the potentially rich source of information—analogue to NMR line shape studies—that can be acquired from nuclear spin relaxation studies of lipid bilayers has not been fully explored to date. Yet recent progress indicates a surprisingly simple picture is possible in terms of viscoelastic properties of the membrane lipids.⁶⁵ This viewpoint assumes one is prepared to relinquish an inherently molecular interpretation, as implicit in many of the current paradigms of structural biology, in favor of a continuum picture drawn from material science. Clearly, the information from ^2H NMR is site-specific in that individual C— ^2H positions are observed. On the other hand, the relatively long spectroscopic time scale ($\sim 10^{-6}$ s) means that the quantities are averaged over a distribution of molecular sites.⁴ It is both the strength and the weakness of such an approach^{15,16} that it does not rest upon any specific molecular details.

Collective Bilayer Deformations. For lipid bilayers in the fluid phase, interpretation of the observables from ^2H NMR spectroscopy, viz., the profiles of the R_{1Z} rates and S_{CD} order parameters, leads naturally to a picture in which the collection of bilayer lipids is considered, rather than the individual molecules.²⁵ To gain a more physical picture of the bilayer dynamics, it is useful to inquire further as to the lengths over which the elastic disturbances can occur. The $\omega^{-1/2}$ frequency dependence observed in the megahertz regime suggests the deformation modes encompass Fourier component wavelengths on the order of about the bilayer thickness and less.¹⁶ Following Bloom et al.,⁴ we refer to such material properties as involving the mesoscopic length scale of ~ 1 – 100 nm, intermediate between the macroscopic bilayer (≥ 500 nm) and the microscopic dimensions, that is, corresponding to the individual flexible molecules (≤ 1 nm). Our experimental findings suggest that the NMR relaxation of fluid bilayers (L_α phase) is governed by a broad distribution of thermal membrane fluctuations. These

fluctuations originate from collective excitations of the quasi-elastic fluid, due to tethering of the lipids to the aqueous interface via their polar headgroups. The relatively slow motions can include collective bilayer excitations, formulated as order-director fluctuations (ODF), together with effective rotations of the flexible lipid molecules.^{25,65} Depending on the wavelength in relation to the interlamellar spacing, quasi-coherent fluctuations of either a 3-D (splay, twist, and bend) or a 2-D (splay) nature are possible.^{15,16,25,43,44,66} We propose that the entire fluctuation spectrum is important for interbilayer repulsions (due to entropic confinement)^{6,37,67} and that all the modes should be considered unless they are unrelated to the biochemical or biophysical properties of interest. Clearly, such a continuum elastic picture represents a significant departure from molecular theories for lipid bilayer relaxation.^{15,33,34} One should note that the model does not preclude—and ultimately must reside in—a molecularly specific interpretation of the material parameters.⁶⁸

It may be surprising that our results for complicated lipid bilayer systems, involving flexible molecules with many internal degrees of freedom, can be understood in terms of fairly simple concepts drawn from material science. The reason the R_{1Z} relaxation is influenced by small-amplitude, collective order fluctuations in the liquid-crystalline (L_α) phase is that the local segmental motions of the lipids are very fast ($\tau_c \approx 10^{-11}$ s), with spectral densities extending to very high frequencies.^{12,16} Consequently, in lipid bilayers, slower, quasi-coherent order fluctuations in the nanosecond range can provide a frequency-dependent relaxation enhancement versus simple n -paraffinic liquids, for example, n -hexadecane. From the value²⁵ of $R_{1Z}^{\text{int}} \approx 12.3 \text{ s}^{-1}$, the correlation times for the internal (local) chain motions are estimated using NMR relaxation theory¹² to be in the range of ~ 30 ps. It follows that the contributions from local acyl chain fluctuations, for example, *trans*–*gauche* isomerizations, are relatively small in all cases. We note that the square-law plots for the various liquid-crystalline bilayers have rather similar ordinate intercepts, which given our framework implies the rate of the local segmental motions, that is, bilayer microviscosity, is similar for the systems studied. These conclusions are generally consistent with all-atom molecular dynamics simulations of lipid bilayers in the L_α state.⁵⁹ They emphasize the concept of the membrane as an ordered fluid, involving the effective grafting of the phospholipid molecules to the aqueous interface via their polar headgroups, whereas the bilayer interior is essentially liquid hydrocarbon.

A Membrane Elastometer on the Mesoscopic Length Scale. How can one further interpret the rich and seemingly contradictory influences of the various membrane constituents on the two spectroscopic observables? Clearly, such behavior is difficult to rationalize in the absence of an appropriate paradigm. Given the above framework, the R_{1Z} rates for different bilayer systems can be compared by using the S_{CD} order parameters for a given segment as a “reference” to gain an idea of their relative softness in the liquid crystalline (L_α) state. For the various bilayers studied, the ^2H R_{1Z} rates for comparable S_{CD} values—related to the bilayer softness—follow the rank order $\text{DMPC}/\text{C}_{12}\text{E}_8 > \text{DLPC} \approx \text{DMPC} \approx \text{DPPC} \approx \text{DSPC} > \text{DPPE}$

(55) Nagle, J. F.; Zhang, R. T.; Tristram-Nagle, S.; Sun, W. J.; Petrache, H. I.; Suter, R. M. *Biophys. J.* **1996**, *70*, 1419–1431.

(56) Petrache, H. I.; Gouliavaev, N.; Tristram-Nagle, S.; Zhang, R.; Suter, R. M.; Nagle, J. F. *Phys. Rev. E* **1998**, *57*, 7014–7024.

(57) Nagle, J. F.; Tristram-Nagle, S. *Curr. Opin. Struct. Biol.* **2000**, *10*, 474–480.

(58) Nagle, J. F.; Tristram-Nagle, S. *Biochim. Biophys. Acta* **2000**, *1469*, 159–195.

(59) Venable, R. M.; Zhang, Y.; Hardy, B. J.; Pastor, R. W. *Science* **1993**, *262*, 223–226.

(60) Chiu, S. W.; Jakobsson, E.; Subramaniam, S.; Scott, H. L. *Biophys. J.* **1999**, *77*, 2462–2469.

(61) Saiz, L.; Klein, M. L. *Biophys. J.* **2001**, *81*, 204–216.

(62) Huber, T.; Rajamoorthi, K.; Kurze, V. F.; Beyer, K.; Brown, M. F. *J. Am. Chem. Soc.* **2002**, *124*, 298–309.

(63) Klose, G.; Levine, Y. K. *Langmuir* **2000**, *16*, 671–676.

(64) Lindahl, E.; Edholm, O. *J. Chem. Phys.* **2001**, *115*, 4938–4950.

(65) Brown, M. F.; Nevzorov, A. A. *Colloids Surf., A* **1999**, *158*, 281–298.

(66) Althoff, G.; Heaton, N. J.; Gröbner, G.; Prosser, R. S.; Kothe, G. *Colloids Surf., A* **1996**, *115*, 31–37.

(67) McIntosh, T. J. *Curr. Opin. Struct. Biol.* **2000**, *10*, 481–485.

(68) McConnell, H. M. In *Spin Labeling Theory and Applications*; Berliner, L. J., Ed.; Academic Press: New York, 1976; pp 525–560.

> DMPC/cholesterol. In quantitative terms, given a square-law relation, a softer bilayer has a large slope in plots of $R_{1Z}^{(0)}$ versus $|S_{CD}^{(0)}|^2$ and vice versa. The main influence of the lipid composition is on the viscoelastic behavior as manifested by the slope, whereas the ordinate intercept is similar for all the bilayers studied. In fact, one does not even need a square-law functional dependence of the two observables along the entire acyl chain to draw useful inferences about the bilayer flexibility.

One expects the bilayer softness, viz., elasticity, to depend on both the area per lipid and the lipid acyl length. First, let us consider the homologous series of diacylphosphatidylcholines, with a fully methylated quaternary nitrogen headgroup. For the homologous PCs, Petrache et al.^{38,69} have shown that as the lipid acyl length increases, there is only a small contraction of the aqueous interfacial area, so that the bilayer thickness increases for longer chains. In this case, both the S_{CD} and the R_{1Z} values depend on the variables of acyl position and acyl length, as well as temperature. For instance, both S_{CD} and R_{1Z} decrease with the acyl segment position away from the polar headgroup—the well-established order and relaxation profiles.^{17,39} Moreover, for a given segment position, both S_{CD} and R_{1Z} decrease with increasing temperature. Yet for the same value of S_{CD} , one has a similar value of R_{1Z} , indicating a correlation of the two spectroscopic observables (cf. Results). Given a composite membrane deformation model, for the PCs there appear to be only minor influences of either temperature or the bilayer thickness on the viscoelastic constant D . Provided the viscosity η governing the modes is about the same, the (single) elastic constant K is similarly unaltered, which describes the force needed for deformation. For splay deformations, multiplying by the bilayer thickness gives the so-called bending rigidity κ , indicating that the deformation energy increases with the thickness of the bilayer film. Consequently, at approximately constant area, the flexibility or dynamical softness of phosphatidylcholines becomes smaller with increasing acyl length, in accord with physical intuition.

Next we consider phosphatidylethanolamine (PE), in which the headgroup nitrogen is a primary amine. The absence of methylation as for PC means the headgroup is smaller, which additionally can engage in hydrogen bonding involving the ammonium nitrogen and the phosphate oxygens. For bilayers of PE, there is an *increase* in the values of the S_{CD} order parameters.⁵⁴ By contrast, a *decrease* is evident in the R_{1Z} rates versus the PC series—thus the spectral density is shifted to higher frequencies. This implies that bilayers containing PE are less flexible than in the case of PC and that this increase in bilayer stiffness is a consequence of the presence of PE in membranes. The reduction in the viscoelastic constant D for PE versus PC corresponds to an increase in the elastic constant K . Consequently, it is plausible that nature has selected PE as a means of stiffening the bilayer in the fluid state up to a certain extent. Increased rigidity of bilayers imparted by the presence of PE may play an important biological role, for example, with regard to intra- and interbilayer forces, as well as the interactions of lipids with proteins and peptides implicated in various biological functions.^{1,2,70–77}

Our experimental NMR relaxation studies reveal that the behavior observed upon addition of a cosurfactant such as $C_{12}E_8$ to the bilayer is opposite to the effect of PE. For phosphatidylcholine bilayers containing the nonionic surfactant $C_{12}E_8$, there is a small *decrease* in the S_{CD} values of the various acyl segments, whereas little influence on the segmental R_{1Z} rates is found.⁷⁸ Thus, a larger value of the segmental R_{1Z} rate is observed for a given order parameter S_{CD} than that in the absence of cosurfactant. This observation implies that the spectral density is shifted from higher to lower frequencies by the presence of detergent, corresponding to a reduction in the elastic constant K . According to the composite model, the bilayer is now softer and more flexible due to the presence of a cosurfactant. By contrast, for cholesterol-containing bilayers, an *increase* in the S_{CD} order parameters is seen versus PC alone, accompanied by an opposite *decrease* in the R_{1Z} rates. Such behavior is qualitatively similar to the effect of PE, although the magnitude is greater.

To explain these findings, viz., the opposite effects of PE and cholesterol, on one hand, versus a nonionic surfactant, on the other, we propose the following. As noted above, for constant acyl length we expect that the bilayer elasticity is related to the interfacial area per molecule in the liquid-crystalline state.⁷⁹ Deformation of the bilayer favors a confinement of the acyl chains in the center, and thus a loss of their conformational entropy. Now the area per molecule is inversely correlated with the configurational order of the acyl chains, and hence with their projected length along the bilayer normal.^{23,38,69} Elsewhere we have proposed that the case of PE represents the lateral packing limit of fluid acyl chains.³⁸ For PE-containing bilayers as compared to PC, the smaller interfacial area per lipid gives an increase in the acyl ordering,⁵⁴ corresponding to a stretching of the chains along the bilayer normal. The concomitant reduction in entanglement of the acyl chains is associated with an increase in bilayer stiffness, and possibly a greater rate of effective axial lipid rotations, hence a lessening of the dynamical roughness of the bilayer. That is to say, as the interfacial area per molecule becomes smaller, there is a greater loss of the acyl chain conformational entropy associated with deformation away from the planar state. In consequence, the membrane is less deformable—it becomes stiffer and more resilient to curvature deformation. Moreover, we propose that this increase in the bilayer elastic moduli (stiffness) relative to PC is associated with a weaker repulsive force between PE-containing bilayers in multilamellar samples. On account of the smaller spectral density due to quasi-coherent elastic modes, there is a reduced entropic pressure, which yields less hydration of the multilamellar membrane dispersion, and a smaller interlamellar separation.⁸⁰ Hence there is a connection between

(69) Petrache, H. I.; Salmon, A.; Brown, M. F. *J. Am. Chem. Soc.* **2001**, *123*, 12611–12622.

(70) Navarro, J.; Toivio-Kinnucan, M.; Racker, E. *Biochemistry* **1984**, *23*, 130–135.

(71) Jensen, J. W.; Schutzbach, J. S. *Biochemistry* **1984**, *23*, 1115–1119.

(72) Baldwin, P. A.; Hubbell, W. L. *Biochemistry* **1985**, *24*, 2633–2639.

(73) Wiedmann, T. S.; Pates, R. D.; Beach, J. M.; Salmon, A.; Brown, M. F. *Biochemistry* **1988**, *27*, 6469–6474.

(74) Gibson, N. J.; Brown, M. F. *Biochemistry* **1993**, *32*, 2438–2454.

(75) Keller, S. L.; Bezrukov, S. M.; Gruner, S. M.; Tate, M. W.; Vodyanoy, I.; Parsegian, V. A. *Biophys. J.* **1993**, *65*, 23–27.

(76) Lundbaek, J. A.; Maer, A. M.; Andersen, O. S. *Biochemistry* **1997**, *36*, 5695–5701.

(77) Lewis, J. R.; Cafiso, D. S. *Biochemistry* **1999**, *38*, 5932–5938.

(78) Otten, D.; Brown, M. F.; Beyer, K. J. *Phys. Chem. B* **2000**, *104*, 12119–12129.

(79) Szleifer, I.; Kramer, D.; Ben-Shaul, A.; Roux, D.; Gelbart, W. M. *Phys. Rev. Lett.* **1988**, *60*, 1966–1969.

(80) Rand, R. P.; Parsegian, V. A. *Biochim. Biophys. Acta* **1989**, *988*, 351–376.

bilayer properties on the mesoscopic scale, as studied by NMR relaxation, and macroscopic properties of the bulk material.

Similarly, for bilayers containing cholesterol, a reduction in the interfacial area per phospholipid (condensing effect) yields less chain entanglement, and a greater stretching of the chains along the bilayer normal. In either case, the reduced interfacial area per molecule is associated with an increase in bilayer stiffness, with the effect being largest for the highly condensed, cholesterol-containing bilayer. An interesting corollary is that the maximum increase in the bilayer stiffness that can be achieved by nature, while still maintaining a fluid membrane, involves bilayers containing cholesterol in the liquid-ordered state. The bilayer stiffening effect of cholesterol is revealed by a number of studies, including micropipet aspiration,⁵ vesicle shape fluctuations,^{8,51} and NMR transverse relaxation.⁶⁶ Additional ²H NMR relaxation studies have yielded insights into the basis for the micromechanical properties of the bilayer imparted by this sterol.^{24,65} Moreover, incoherent quasi-elastic neutron scattering studies have suggested that cholesterol protrudes dynamically between the opposing monolayers, thereby increasing the frictional drag which may increase the bilayer elastic curvature modulus.⁸¹

By contrast, inclusion of a single chain amphiphile such as C₁₂E₈ (or lysophosphatidylcholine) yields an opposite increase in the bilayer flexibility, that is, softness, as inferred from NMR relaxation. In this case, the bilayer surface is expanded; there is an increase in the interfacial area per phospholipid molecule, due to the increased configurational freedom and entanglement of the acyl chains (configurational entropy).⁷⁸ This yields a more deformable bilayer, having a concomitantly reduced elastic constant, in agreement with other physicochemical studies of surfactant-containing bilayers. According to studies of macroscopic bilayer deformation, the addition of a cosurfactant gives a decrease in the bending rigidity of lamellar phases of surfactants and phospholipids, involving longer fluctuation wavelengths.⁸ Such a reduction in the bilayer elastic constant due to a cosurfactant yields an increase in entropic repulsion between the lamellae, accompanied by a greater hydration of the membrane dispersion,⁷⁸ analogous to the swelling of dilute lamellar phases of nonionic surfactants.⁸² The increased bilayer flexibility due to a cosurfactant such as C₁₂E₈ is biologically important, for example, in the case of lysophosphatidylcholine,³⁶ and finds practical utility in the solubilization of membrane proteins. Qualitatively, the opposite influences of membrane additives such as a cosurfactant (C₁₂E₈) and cholesterol, as investigated by NMR relaxation (this work), are in good agreement with previous macroscopic studies of bilayer deformation,^{8,51,83} and support the physical significance of the model.

Material Constants—Influences of Lipid Composition.

Given the above continuum elastic picture, the biophysical relevance of these findings can be further expanded as follows. For the purposes of illustration, the plausible range of the viscoelastic parameters obtained from NMR enables one to make heuristic estimates of the so-called bending rigidity κ of the bilayer, in analogy with the properties of bulk systems. With

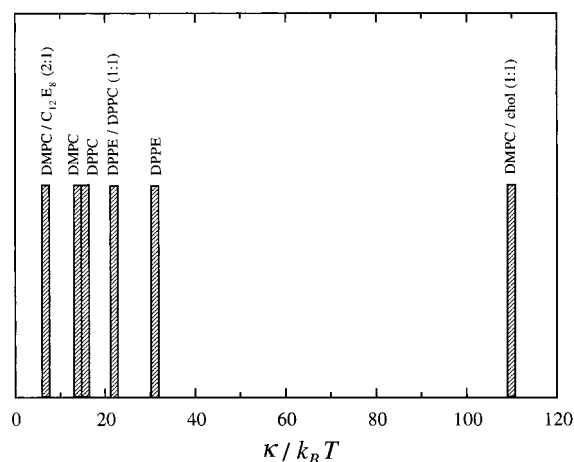


Figure 7. Estimated bending rigidity κ from ²H NMR relaxation data, showing influences of the lipid composition on bilayer softness in the fluid state. Note that inclusion of C₁₂E₈ yields a significant reduction in κ versus phosphatidylcholines such as DMPC and DPPC. Replacement of PC headgroups by PE leads to a dramatic increase in bilayer rigidity, and the inclusion of cholesterol produces the stiffest bilayer of all.

use of the composite deformation model (cf. Results), one obtains estimates of κ that fall in the range of micromechanical studies of membrane deformation,^{5,36,50} as well as vesicle fluctuation experiments.⁵¹ Figure 7 shows a summary of the estimates of κ obtained from our ²H R₁₂ relaxation studies of various bilayers, which can be thought of as furnishing a scale of bilayer softness. As discussed by Olsson and Wennerström,⁸² nonionic surfactants form extremely soft bilayers. According to Figure 7, the addition of a cosurfactant such as C₁₂E₈ yields a reduction in the value of κ . Hence the presence of a surfactant with a single hydrocarbon chain gives an increased flexibility of the mixed bilayer versus pure phosphatidylcholines, such as DMPC and DPPC. On the other hand, the presence of PE headgroups yields an appreciable stiffening of the bilayer, as manifested by the estimates of κ . Last, Figure 7 shows that of all the membrane additives studied, cholesterol is unique in that it produces the stiffest bilayer of all; that is, the liquid-ordered phase has the largest values of the bending rigidity κ , while still maintaining a fluid bilayer. The effects of bilayer additives observed with NMR relaxation, an inherently site-specific technique, agree with macroscopic studies of bilayer elasticity, thus reinforcing our hypothesis of an effectively continuous distribution of bilayer excitations.¹⁵ Clearly, the above findings support one of the major novel aspects of the present work, viz., extension of the concept of membrane elasticity to relatively short distances, encompassing the mesoscopic regime. Moreover, they emphasize that the relaxation behavior is associated with the collection of lipid molecules, rather than the intrinsic motions of the individual lipids.

Conclusions and Biophysical Significance

In this article, we describe a novel approach for investigating the elastic properties of membrane lipid bilayers. By correlating the NMR relaxation rates of the phospholipid molecules with their order profiles, we obtain information pertinent to the forces associated with the bilayer deformation. This work provides striking new evidence that the elastic deformations of lipid membranes encompass a range of length and time scales in the liquid-crystalline (*L_α*) state. Our experimental findings imply

(81) Gliss, C.; Randel, O.; Casalta, H.; Sackmann, E.; Zorn, R.; Bayerl, T. *Biophys. J.* **1999**, *77*, 331–340.

(82) Olsson, U.; Wennerström, H. *Adv. Colloid Interface Sci.* **1994**, *49*, 113–146.

(83) Auguste, F.; Barois, P.; Fredon, L.; Clin, B.; Dufourc, E. J.; Bellocq, A. *M. J. Phys. II* **1994**, *4*, 2197–2214.

that quasi-coherent order fluctuations are already present in lipid bilayers involving lengths on the order of about the bilayer thickness and even less. A hierarchical superposition of relaxation modes is suggested, ranging from 2-D collective undulations at lower frequencies, to 3-D collective fluctuations at higher frequencies, and finally terminating with noncollective molecular protrusions from the bilayer and local segmental motions of the flexible lipids. Within this framework, the NMR relaxation data show clear influences of the bilayer thickness (lipid acyl length), the interfacial area per molecule (polar headgroup), and additives such as nonionic detergents and cholesterol. A scale of bilayer softness is evident, ranging from highly deformable, mixed phosphatidylcholine/surfactant systems to systems containing phosphatidylethanolamine with an increased bilayer stiffness, and ultimately the very rigid yet fluid bilayers containing cholesterol. Our theoretical interpretation of the NMR relaxation data correlates well with previous macroscopic studies of membrane bending deformations. Hence we propose a connection between the microscopic and mesoscopic behavior of lipids as studied with NMR relaxation and the elastic properties of the bilayer on the macroscopic scale. Last, we suggest the softness of membrane bilayers is associated with the lipid diversity of natural biomembranes, for example, in relation to the forces associated with their microstructure, as well as lipid–protein interactions implicated in key biological functions.

Acknowledgment. This work was supported by the Röntgen-Professorship of Physics at the University of Würzburg and by the Volkswagen-Stiftung (M.F.B.). Additional support was provided by the U.S. National Institutes of Health (M.F.B.), a postdoctoral fellowship from the U.S. NIH (R.L.T.), a stipend from the Deutsche Akademische Austauschdienst (D.O.), and by the Deutsche Forschungsgemeinschaft (K.B.). Part of this work was conducted at the University of Würzburg, and one of us (M.F.B.) is grateful to Profs. Thomas Bayerl, Axel Haase, and Gottfried Landwehr for their generous hospitality. Finally, we also thank Myer Bloom, Thomas Huber, Gary Martinez, John Nagle, and Horia Petrache for many helpful discussions.

Appendix: Composite Model for Structural Dynamics of Lipid Bilayers

Here, we provide a brief description of the models employed for the analysis of solid-state ^2H NMR relaxation data for membrane lipid bilayers in the liquid-crystalline (L_α) state. Let us assume a continuum framework, in which the bilayer interior is modeled in terms of a local director field.^{15,16} According to this treatment, rapid local motions of the *static* EFG tensor can occur with respect to an internal frame, described by a fast order parameter $S_f^{(2)} = \langle D_{00}^{(2)}(\Omega_{PI}) \rangle$. Moreover, slower motions of the *residual* EFG tensor remaining or left-over from the faster fluctuations can take place. After transforming from the internal frame to the molecular frame, the slow order parameter is given by $S_s^{(2)} = S_s^{(2)\text{mol}} S_s^{(2)\text{col}} = \langle D_{00}^{(2)}(\Omega_{MN}) \rangle \langle D_{00}^{(2)}(\Omega_{ND}) \rangle$ which can include the combined effects of molecular and collective motions. (It may be helpful for the reader to refer to a schematic diagram of the various Euler angles, see e.g. ref 12.) Here, the symbol $D_{m'm}^{(2)}(\Omega)$ denotes the rank-2 Wigner rotation matrix elements,¹² where (m' , m) are generalized projection indices. The various Euler angles $\Omega \equiv \Omega_{PI}$, Ω_{IM} , Ω_{MN} , and

Ω_{ND} denote, respectively, transformation from the principal axis system (P) of the EFG tensor to an internal frame (I); from the internal frame to the molecular frame (M); from the molecular frame to the local or instantaneous director frame (N); and finally from the local director to the average director frame (D), coinciding with the macroscopic bilayer normal.²² According to the closure property of the rotation group, the observed order parameter is given by $S_{\text{CD}} = S_f^{(2)} \tilde{S}_{\text{int}}^{(2)} S_s^{(2)}$, where $\tilde{S}_{\text{int}}^{(2)} \equiv \{D_{00}^{(2)}(\Omega_{IM}) - \sqrt{2/3} \eta_Q^{\text{eff}} \text{Re} D_{\pm 20}^{(2)}(\Omega_{IM})\}$ is a geometric factor that relates the principal axis systems of the comparatively fast and slow motions.

Our development assumes a composite stochastic process, which explains both the orientation dependence and the frequency (magnetic field) dependence of the R_{1Z} and R_{1Q} relaxation rates of bilayer lipids in the liquid-crystalline state.²⁵ According to ref 25, the irreducible spectral densities due to relatively slow motions are given by:

$$J_m(\omega) = J_m^{\text{col}}(\omega) + J_m^{\text{mol}}(\omega) + J_m^{\text{mol-col}}(\omega) \quad (\text{A1})$$

in which ω is the angular frequency. The above decomposition considers collective (col) and molecular (mol) motions separately, together with a geometric (mol-col) cross term between the various rotational modes and the collective deformations. In eq A1, the first term represents the spectral density due to 3-D collective membrane deformations and assumes a single elastic constant for splay, twist, and bend excitations. Assuming small-amplitude order-director fluctuations (linear order),^{22,25} we have that

$$J_m^{\text{col}}(\omega) = \frac{5}{2} S_{\text{CD}}^2 D \omega^{-(2-d/2)} [|D_{-1m}^{(2)}(\Omega_{\text{DL}})|^2 + |D_{1m}^{(2)}(\Omega_{\text{DL}})|^2] \quad (\text{A2})$$

where d is the dimensionality, and the Euler angles Ω_{DL} describe the fixed transformation from the director frame (D), viz., the macroscopic bilayer normal, to the laboratory frame (L). The above formula corresponds to the overdamped regime for collective motions—each of the modes relaxes with a single exponential time constant, and oscillatory behavior is not considered. According to eq 5, the spectral densities $J_m^{\text{col}}(\omega)$ depend on the square of the observed order parameter S_{CD} . The viscoelastic constant is given by $D = 3k_B T \sqrt{\eta} / 5\pi \sqrt{2K^3 (S_s^{(2)\text{col}})^2}$, where a single elastic constant K is assumed for the various bilayer deformations, η is the corresponding viscosity coefficient, and the other symbols have their conventional meanings. (Note that the slow order parameter $S_s^{(2)\text{col}}$ is absorbed into the viscoelastic constant D and cannot be determined independently of K and η .) Thus, a square-law functional dependence of the spectral densities and relaxation rates on the observed order parameter S_{CD} is predicted for collective membrane motions, provided $S_s^{(2)\text{col}}$ and the geometric factor $\tilde{S}_{\text{int}}^{(2)}$ are constant along the entire chain.¹⁵ For the case of 3-D director fluctuations ($d = 3$), an $\omega^{-1/2}$ frequency dispersion is obtained as a characteristic hallmark. (One can also consider 2-D membrane deformations ($d = 2$), e.g., in terms of a flexible surface model, leading to an ω^{-1} frequency dependence,^{66,84} which is not observed experimentally at megahertz frequencies.²²)

(84) Marqusee, J. A.; Warner, M.; Dill, K. A. *J. Chem. Phys.* **1984**, *81*, 6404–6405.

The second term in eq A1 corresponds to the spectral densities for rotations of the flexible lipid molecules and is given by:²⁴

$$J_m^{\text{mol}}(\omega) = \frac{S_{\text{CD}}^2}{\tilde{S}_{\text{int}}^{(2)2} S_s^{(2)2}} \sum_q \sum_n |D_{0q}^{(2)}(\Omega_{\text{IM}})|^2 - \frac{\eta_{\text{Q}}^{\text{eff}}}{\sqrt{6}} [D_{-2q}^{(2)}(\Omega_{\text{IM}}) + D_{2q}^{(2)}(\Omega_{\text{IM}})]^2 [\langle |D_{qn}^{(2)}(\Omega_{\text{MD}})|^2 \rangle - \langle D_{qn}^{(2)}(\Omega_{\text{MD}}) \rangle^2 \delta_{q0} \delta_{n0}] j_{qn}^{(2)}(\omega) |D_{nm}^{(2)}(\Omega_{\text{DL}})|^2 \quad (\text{A3})$$

Here, the fast order parameter is $S_f^{(2)} = S_{\text{CD}}/\tilde{S}_{\text{int}}^{(2)} S_s^{(2)}$, which is related to the effective quadrupolar coupling constant by $\chi_{\text{Q}}^{\text{eff}} = \chi_{\text{Q}} S_f^{(2)}$, and $\eta_{\text{Q}}^{\text{eff}}$ is the effective asymmetry parameter of the residual EFG tensor (due to pre-averaging by faster segmental motions). The Euler angles $\Omega \equiv \Omega_{\text{MD}}$ refer to transformation from the molecular frame (M) to the director frame (D), where the (projection) indices q and n describe rotations about the molecular long axis and the director, respectively. The quantities $j_{qn}^{(2)}(\omega)$ denote Lorentzian reduced spectral densities, with correlation times τ_{qn} corresponding to the principal values of the rotational diffusion tensor, D_{\perp} and D_{\parallel} .^{15,29} Assuming that off-axis motions are negligible,²⁵ that is, $S_s^{(2)\text{mol}} \rightarrow 1$, then $\tau_{qn} = 1/D_{\parallel} q^2$. Last, the geometrical cross term in eq A1 is given by:²⁴

$$J_m^{\text{mol-col}}(\omega) = \frac{S_{\text{CD}}^2}{\tilde{S}_{\text{int}}^{(2)2} S_s^{(2)2}} \sum_q |D_{0q}^{(2)}(\Omega_{\text{IM}})|^2 - \frac{\eta_{\text{Q}}^{\text{eff}}}{\sqrt{6}} [D_{-2q}^{(2)}(\Omega_{\text{IM}}) + D_{2q}^{(2)}(\Omega_{\text{IM}})]^2 \times \{ J_{q1}^{\text{mol-col}}(\omega) [3|D_{0m}^{(2)}(\Omega_{\text{DL}})|^2 + |D_{-2m}^{(2)}(\Omega_{\text{DL}})|^2 + |D_{2m}^{(2)}(\Omega_{\text{DL}})|^2] + \left[\frac{3}{2} J_{q0}^{\text{mol-col}}(\omega) + J_{q2}^{\text{mol-col}}(\omega) \right] \times [|D_{-1m}^{(2)}(\Omega_{\text{DL}})|^2 + |D_{1m}^{(2)}(\Omega_{\text{DL}})|^2] \} \quad (\text{A4})$$

In the above formula, the individual spectral densities $J_{qn}^{\text{mol-col}}(\omega)$ are Fourier transforms of products of the correlation functions for the various rotational modes (q, n) and the correlation functions for collective membrane deformations, and depend on both K and τ_{qn} .²⁵

According to eqs A2–A4, the various spectral densities in closed form all depend on the square of the segmental order parameter S_{CD} , as a signature of order fluctuations due to comparatively slow motions.¹² Detailed investigations of the model DMPC-*d*₅₄ bilayer have utilized the above formalism to simulate both the frequency (magnetic field) dependence and the angular anisotropy of the relaxation simultaneously.²⁵ Specifically, eq A2 predicts a square-law functional dependence of the $R_{1Z}^{(i)}$ and $R_{1Q}^{(i)}$ relaxation rates on the observed order parameters $|S_{\text{CD}}^{(i)}|$, provided the amplitude of the collective motions as described by $S_s^{(2)\text{col}}$ is the same throughout the bilayer hydrocarbon region.¹⁵ In addition, eqs A3 and A4 require that the amplitude of the relatively slow molecular motions as described by $S_s^{(2)\text{mol}}$ together with the geometric factor $\tilde{S}_{\text{int}}^{(2)}$ does not depend appreciably on the chain position. Any deviation from linearity (upward or downward curvature) can represent variations in the residual coupling tensor along the chain or the amplitude of the comparatively slow motions, that is, alteration of the local director field within the membrane (due to the polar headgroups, double bonds, etc.). The theory predicts the slope of the square-law plots is related to the bilayer deformability, viz., the combined amplitudes of the deformation modes near the resonance frequency (ω_{D} and $2\omega_{\text{D}}$). A simple physical picture is that the splay elastic constant K_{11} (in terms of force) is related to the corresponding splay modulus κ (in terms of energy) by $\kappa = K_{11}t$, where t is the bilayer thickness. The small ordinate intercept represents the contribution from local segmental motions of the chains and is related to the bilayer microviscosity.

JA012660P